Activin B Induces Noncanonical SMAD1/5/8 Signaling via BMP Type I Receptors in Hepatocytes: Evidence for a Role in Hepcidin Induction by Inflammation in Male Mice

Susanna Canali, Amanda B. Core, Kimberly B. Zumbrennen-Bullough, Maria Merkulova, Chia-Yu Wang, Alan L. Schneyer, Antonello Pietrangelo, and Jodie L. Babitt

Program in Anemia Signaling Research (S.C., A.B.C., K.B.Z.-B., M.M., C.-Y.W., J.L.B.), Division of Nephrology, Program in Membrane Biology, Center for Systems Biology, Massachusetts General Hospital, Harvard Medical School, Boston, Massachusetts 02114; Center for Hemochromatosis (S.C., A.P.), University Hospital of Modena and Reggio Emilia, Modena Italy 41124; and Department of Veterinary and Animal Science (A.S.), University of Massachusetts Amherst, Amherst, Massachusetts 01003

Induction of the iron regulatory hormone hepcidin contributes to the anemia of inflammation. Bone morphogenetic protein 6 (BMP6) signaling is a central regulator of hepcidin expression in the liver. Recently, the TGF-β/BMP superfamily member activin B was implicated in hepcidin induction by inflammation via noncanonical SMAD1/5/8 signaling, but its mechanism of action and functional significance in vivo remain uncertain. Here, we show that low concentrations of activin B, but not activin A, stimulate prolonged SMAD1/5/8 signaling and hepcidin expression in liver cells to a similar degree as canonical SMAD2/3 signaling, and with similar or modestly reduced potency compared with BMP6. Activin B stimulates hepcidin via classical activin type II receptors ACVR2A and ACVR2B, noncanonical BMP type I receptors activin receptor-like kinase 2 and activin receptor-like kinase 3, and SMAD5. The coreceptor hemojuvelin binds to activin B and facilitates activin B-SMAD1/5/8 signaling. Activin B-SMAD1/5/8 signaling has some selectivity for hepatocyte-derived cells and is not enabled by hemojuvelin in other cell types. Liver activin B mRNA expression is up-regulated in multiple mouse models of inflammation associated with increased hepcidin and hypoferremia, including lipopolysaccharide, turpentine, and heat-killed *Brucella abortus* models. Finally, the activin inhibitor follistatin-315 blunts hepcidin induction by lipopolysaccharide or *B. abortus* in mice. Our data elucidate a novel mechanism for noncanonical SMAD activation and support a likely functional role for activin B in hepcidin stimulation during inflammation in vivo. **(*Endocrinology* 157: 1146–1162, 2016)**

Functional iron deficiency is a hallmark of anemia of inflammation and is caused by elevated levels of the iron regulatory hormone hepcidin (1). Secreted by the liver, hepcidin induces degradation of the iron exporter ferroportin to limit iron entry into the bloodstream from dietary sources, iron-recycling macrophages, and hepatocyte stores (2). Hepcidin induction during inflammation is partly due to direct transcriptional regulation by the IL-6/signal transducer and activator of transcription 3 (STAT3) pathway (3–5). However, dependence on TGF-β superfamily signaling has also been demonstrated (6–13).

ISSN Print 0013-7227 ISSN Online 1945-7170
Printed in USA

Received August 21, 2015. Accepted December 31, 2015.
First Published Online January 6, 2016

Abbreviations: ACVR, Activin receptor; ALK, Activin receptor-like kinase; BA, *Brucella abortus*; BMP, bone morphogenetic protein; BRE, BMP-responsive element; BRE-Luc, BMP-responsive luciferase reporter; *Dmt1*, divalent metal transporter 1; FBS, fetal bovine serum; *Fpn*, ferroportin; FST315, follistatin-315; GDF, growth and differentiation factor; Hep-Luc, hepcidin promoter firefly luciferase reporter; HJV, hemojuvelin; HJV.Fc, HJV extracellular domain fused to the IgG Fc fragment; IMCD, inner medullary collecting duct; LPS, lipopolysaccharide; P-SMAD, phosphorylated-SMAD; qRT-PCR, quantitative real-time PCR; R-SMAD, receptor-activated SMAD; RGM, repulsive guidance molecule; siRNA, small interfering RNA; SPR, surface plasmon resonance; STAT3, signal transducer and activator of transcription 3; TBS-T, 50mM Tris (pH 7.4), 150mM NaCl, and 0.05% Tween 20; WT, wild type.

The TGF-β superfamily of signaling molecules, including TGF-βs, bone morphogenetic proteins (BMPs), and activins, participate in a diverse array of biological functions by binding to complexes of type II and type I serine threonine kinase receptors to induce phosphorylation of receptor-activated SMADs (R-SMADs) (14–15). Phosphorylated R-SMADs complex with SMAD4, translocate to the nucleus, and regulate gene transcription. Typically, different ligand subfamilies signal via distinct, but overlapping subsets of receptors and R-SMADs. In particular, BMPs use type II receptors BMPR2, ACVR2A, and ACVR2B, type I receptors ALK1, ALK2, ALK3, and ALK6, and R-SMADs 1, 5, and 8, whereas TGF-βs use the type II receptor TGFBR2, the type I receptor ALK5, and R-SMADs 2 and 3 (14, 15). Activins use type II receptors that overlap with the BMP subfamily (ACVR2A and ACVR2B), but distinct type I receptors (ALK4 and ALK7), and share R-SMAD2/3 with the TGF-β subfamily (14, 15). Numerous other regulatory mechanisms exist to fine tune this canonical signaling pathway, including coreceptors to modify ligand-receptor binding (14, 15).

Mouse and human genetic studies have established that the ligand BMP6 (16, 17), type II receptors ACVR2A and BMPR2 (18), type I receptors ALK2 and ALK3 (19), coreceptor hemojuvelin (HJV) (20–23), and SMAD4 (7) are critical regulators of hepcidin expression and systemic iron balance, because global or liver-specific knockout/mutation of these molecules leads to hepcidin deficiency and iron overload. Liver BMP6-SMAD1/5/8 signaling is stimulated by iron (24, 25) and induces hepcidin transcription directly via specific BMP-responsive elements (BREs) on the hepcidin promoter (26, 27).

SMAD1/5/8 signaling also has a role in hepcidin regulation during inflammation (6), because blocking this pathway with soluble HJV or a small molecule BMP type I receptor inhibitor blunts hepcidin induction, increases iron availability, and ameliorates anemia in animal models of anemia of inflammation (7–11). Notably, these SMAD1/5/8 pathway inhibitors do not impact the inflammatory response or the induction of liver STAT3 phosphorylation (7–11), which are also critical mediators of hepcidin induction by inflammation (3–5). Thus, an intact SMAD1/5/8 pathway is required for the IL-6/STAT3 pathway to maximally stimulate hepcidin. Importantly, this appears to be independent of BMP6, because hepcidin induction by lipopolysaccharide (LPS) is preserved in *Bmp6* null mice (17). One mechanism proposed for the cross talk between these pathways is an interaction at the hepcidin promoter, where the STAT3 binding element is adjacent to the proximal BRE (12). Recently, Besson-Fournier et al (13) proposed activin B as another mechanism of cross talk when they demonstrated increased liver activin B expression in LPS treated mice. Although previously understood to signal via the SMAD2/3 pathway, activin B was shown to increase noncanonical phosphorylated-SMAD (P-SMAD)1/5/8 and hepcidin expression in cultured liver cells (13).

Although Besson-Fournier et al (13) raised an intriguing hypothesis, the molecular mechanisms by which activin B induces noncanonical SMAD1/5/8 phosphorylation and hepcidin expression, the generalizability of activin B-SMAD1/5/8 signaling to other cell systems, and the functional significance of activin B in hepcidin regulation in vivo remain uncertain. Several other non-BMP TGF-β superfamily members were also demonstrated to stimulate hepcidin expression in hepatocyte-derived cells in vitro (7, 9); however, their potency was considerably less than BMP ligands (9). Although the molecular mechanisms for hepcidin induction by these other ligands were not explored, there is increasing recognition that TGF-β superfamily members can crossactivate noncanonical SMAD phosphorylation in certain cellular contexts (28–34). Typically, this noncanonical SMAD phosphorylation requires higher ligand concentrations and is more transient than canonical SMAD phosphorylation (28–32). The molecular mechanisms for this crossactivation are varied, but generally involve canonical type I receptors phosphorylating noncanonical SMADs or heteromeric canonical/noncanonical type I receptor complexes (28–30, 32–34). Although some functional roles for noncanonical SMAD signaling have been described (28–34), there are also reports that P-SMAD1/5/8 stimulated by TGF-β ligands have impaired ability to increase transcription via classical BREs due to the formation of mixed R-SMAD complexes (29, 30). Moreover, although it is difficult to determine TGF-β superfamily ligand concentrations that are physiologically relevant in vivo, because they often act in an autocrine or paracrine fashion, the functional significance of effects that are more transient and require high ligand concentrations may be less certain.

We therefore investigated the dose response and kinetics of activin B stimulation of noncanonical SMAD1/5/8 signaling and hepcidin expression vs canonical SMAD2/3 signaling compared with the related ligand activin A (65% homology) and the main endogenous hepcidin regulator BMP6 in liver cells. We also delineated the detailed molecular mechanisms by which activin B stimulates hepcidin expression using siRNA knockdown of individual canonical and noncanonical signaling pathway components, pull-down experiments, and surface plasmon resonance (SPR). We then examined whether SMAD1/5/8 activation by activin B is selective for liver cells or generalizable to other cell types, and whether HJV or its related coreceptors enable activin B-SMAD1/5/8 signaling. Finally, we

investigated the functional role of activin B in hepcidin regulation under basal conditions and during inflammation in vivo by testing the effects of the activin inhibitor follistatin-315 (FST315) in mice treated without or with LPS or heat-killed *Brucella abortus* (BA).

Materials and Methods

FST315 production

Myc-tagged FST315 was purified from the media of transfected 293-T cells, and protein purity and concentration were determined essentially as described (35).

Animals

Animal protocols were approved by the Institutional Animal Care and Use Committee at Massachusetts General Hospital. HJV knockout (*Hjv*−/−) mice on a C57BL/6 background were kindly provided by Paul Schmidt and Nancy Andrews (23). Primary hepatocytes from *Hjv*−/− and littermate wild-type (WT) mice were isolated as described below. Eight-week-old C57BL/6 male mice (Taconic) received an ip injection of LPS (serotype 055:B5; Sigma) (1 μg/g body weight) or heat-killed BA (1×10^8 particles/mouse; National Veterinary Services Laboratories) (36) with or without 50-μg FST315 in PBS or PBS alone. Alternatively, mice received a sc intrascapular injection of oil of turpentine (5 mL/kg; Sigma) or PBS under isoflurane anesthesia (11). Mice were killed at the indicated times 4 hours to 11 days after injection.

Iron analysis

Serum iron and unsaturated iron binding capacity were measured by colorimetric assay (Pointe Scientific), and transferrin saturation was calculated as described previously (9).

Cell culture, transfection, and luciferase assays

Human hepatoma Hep3B, ovarian granulosa tumor KGN, and mouse renal inner medullary collecting duct (IMCD) cells were cultured as previously described (21, 37, 38). Mouse myoblast C2C12 cells stably expressing a BMP-responsive luciferase reporter (BRE-Luc) (39) provided by Daniel Rifkin (40) were cultured in DMEM with 10% fetal bovine serum (FBS). Mouse primary hepatocytes were isolated by the Massachusetts General Hospital Cell, Tissue and Organ Resource Core. In brief, livers were perfused through the portal vein in situ with 400 mL of perfusion buffer with 1mM EDTA at 4–5 mL/min. The perfusate was equilibrated with 5-L/min 95% O_2 and 5% CO_2 through 5 m of silicone tubing and was maintained by a 100-mm heat exchanger at 37°C before entering the liver. The liver was subsequently perfused with 200 mL of 0.05% collagenase (Sigma) in perfusion buffer with 5mM calcium chloride at the same flow rate. The resulting cell suspension was filtered through 2 nylon meshes with grid sizes 250 and 62 pm (Small Parts). The cell pellet was collected by centrifugation at 50 g for 5 minutes. After centrifugation, the cells were gently washed with culture medium (DMEM powered with 10% FBS, 2% penicillin/streptomycin, 0.5-U/mL insulin, 7.5-μg/mL hydrocortisone,14-ng/mL glucagon, and 20-ng/mL epidermal growth factor), counted, and plated.

Transfections were performed with Lipofectamine 2000 (Invitrogen) or DharmaFECT1 (Dharmacon; for siRNAs) according to the manufacturer's instructions. siRNA duplexes in annealed and purified form for ALK2, ALK3, ALK6, BMPR2, ACVR2A, and ACVR2B were obtained from Ambion, and sequences were previously described and validated for efficacy and specificity (37). siRNA for SMAD5, SMAD2, SMAD3, ALK4, ALK7, and HJV were obtained from Dharmacon (OnTARGET-Plus siGenome, M-015791-00-0005, M-003561-01-0005, M-020067-00-0005, M-004925-01-0005, M-004929-02-0005, and M-018751-02-0005). Where indicated, cells were transiently transfected with BRE-Luc, a SMAD3 responsive (CAGA-Luc) (41) or a hepcidin promoter firefly luciferase reporter (Hep-Luc) (21) in combination with a control *Renilla* luciferase vector (pRL-TK) (Promega) in a ratio of 10:1 as previously described (21), with or without 40nM siRNAs, with or without cDNA encoding HJV (20–200 ng) (21).

Cells were serum starved with 1% FBS for 24 hours and stimulated with or without 5- or 50-ng/mL activin B, activin A, or BMP6 (R&D Systems), with or without FST315 for 1–24 hours. Serum starvation was initiated 18 hours after plating for primary hepatocytes and 24 hours after transfection. Where indicated, relative luciferase activity was determined by the Dual-Luciferase reporter assay system (Promega) as described previously (21).

Immunoblot

Total or phosphatidylinositol phospholipase C-digested (for HJV immunoblots; Sigma) protein extracts were prepared and immunoblots performed as described previously (42, 43) using antibodies to P-SMAD1/5/8, SMAD1, P-SMAD2, SMAD2, P-STAT3, STAT3, P-SMAD3, and SMAD3 (9511, 9743, 3101, 9517, 9134, 9132, 9520, and 9513; Cell Signaling Technology); mouse HJV (AF3634; R&D Systems); c-Myc (ab19234; Abcam); hemagglutinin (sc-805; Santa Cruz Biotechnology, Inc); and pan-actin (MAB1501R; Millipore) (Supplemental Table 1). During the course of this study, the Cell Signaling P-SMAD1/5/8 antibody was discontinued, and all mouse liver extracts were evaluated using P-SMAD5 and SMAD5 antibodies (ab92698 and ab40771; Abcam) (Supplemental Table 1, validated in Supplemental Figure 1) using a modified protocol. In brief, extracts prepared as described above were separated by SDS-PAGE on a 10% acrylamide gel and transferred to nitrocellulose. Blots were blocked with 5% nonfat dry milk in 50mM Tris (pH 7.4), 150mM NaCl, and 0.05% Tween 20) (TBS-T) for 1 hour at room temperature and incubated with P-SMAD5 antibody at 1:1000 in TBS-T with 5% nonfat dry milk overnight at 4°C. After washing with TBS-T, blots were incubated for 1 hour at room temperature with horseradish peroxidase-conjugated secondary antirabbit antibody (Cell Signaling), washed in TBS-T, and enzymatic activity was visualized using an enhanced chemiluminescence detection kit (GE Healthcare). Blots were stripped and reprobed with SMAD5 antibody (1:2000) using the same protocol. Chemiluminescence quantitation of scanned films was performed using ImageJ 1.46r (44), with all data normalized to total SMAD, STAT3, or actin.

mRNA purification, reverse transcription, and quantitative real-time PCR (qRT-PCR)

Total RNA was isolated using QIAshredder and RNeasy purification kits (QIAGEN), cDNA was synthesized from

1000-ng RNA using the iScript cDNA synthesis kit (Bio-Rad), and qRT-PCR was performed using the Power SYBR Green PCR Master Mix as described previously (45) using primers in Supplemental Table 2. Relative mRNA expression was determined using the ΔΔCt method with *RPL19* as reference as described previously (42).

Pull-down assay

Purified HJV extracellular domain fused to the IgG Fc fragment (HJV.Fc) (5 μg) (9) and activin B (1 μg), either individually or together, were preincubated for 16 hours, incubated with Protein-A beads (Pierce) for 16 hours at 4°C, and proteins were eluted in Laemmli sample buffer as previously described (16). Eluted proteins and solution aliquots before Protein-A pull-down were separated by reducing SDS-PAGE followed by immunoblot using activin B antibody (MAB659; R&D Systems) and human/mouse HJV antibody (AF3720; R&D Systems) (Supplemental Table 1).

Surface plasmon resonance

SPR kinetics experiments were performed on a Biacore T200 (GE Healthcare) essentially as described previously (46) with minor modifications. In brief, carrier-free recombinant human activin B and HJV were obtained from R&D Systems. Activin B was diluted in sodium acetate pH 4.0 (GE Healthcare) and immobilized by the amine coupling method on a CM5 sensor chip to immobilization levels of 300 and 1000 RU. Data obtained from 2 immobilization levels showed no significant difference. HJV was diluted in running buffer HBS-EP+ (GE Healthcare) at concentrations typically ranging from 25nM to 400nM as a series of 5 2-fold escalations with 100nM concentrations run in duplicate in the middle and at the end of each multicycle. The association and dissociation times were 240 and 600 seconds, respectively. The flow rate was 30 μL/min. The sensor surface was regenerated after each binding cycle by consecutive injections of glycine-HCl (pH 2.2) (GE Healthcare) for 60 seconds and then 4M urea, 50mM Tris-HCl (pH 8.0), 150mM NaCl for additional 60 seconds, followed by 100 seconds of stabilization. The kinetic fitting was carried out with Biacore T200 evaluation software by global fitting using 1:1 Langmuir binding model. The Kon (association rate) and Koff (dissociation rate) values were used to calculate K_D = Koff/Kon. Experiments were repeated 3 times, and the mean $K_D \pm$ SE is reported.

Statistics

Statistical significance was determined by 2-tailed Student's *t* test, one- or two-way ANOVA with Dunnett's, Bonferroni, or Tukey post hoc test for pairwise multiple comparisons as indicated using Prism 5 (GraphPad). $P < .05$ was considered significant.

Results

Activin B, but not activin A, stimulates hepcidin expression with similar potency and kinetics as BMP6 in Hep3B cells and primary mouse hepatocytes

The recent report that activin B can stimulate hepcidin expression in HepG2 cells (13) is consistent with previous studies showing that other non-BMP TGF-β superfamily members can stimulate hepcidin expression in hepatocyte-derived cells in vitro (7, 9). However, the potency of other non-BMP ligands to stimulate hepcidin was considerably less than BMP ligands (9). We therefore examined the potency of activin B to stimulate hepcidin expression compared with the known endogenous hepcidin regulator BMP6 and the closest homologue activin A.

Due to concerns that higher ligand concentrations may crossactivate noncanonical SMAD signaling in a way that might not be physiologically relevant, we first performed a dose curve to determine the lowest concentration of activin B that reliably stimulated canonical SMAD2 phosphorylation in Hep3B cells. As shown in Figure 1A, activin B at 5 ng/mL increased SMAD2 phosphorylation by approximately 5-fold, whereas negligible stimulation was seen at 2 ng/mL. A dose-response effect was seen for increasing ligand concentrations up to 25 ng/mL. Similar effects were seen for activin A. Consistent with previous reports that higher ligand concentrations can crossactivate noncanonical SMAD signaling in some cellular contexts (28–34), higher BMP6 concentrations (25 ng/mL) also stimulated SMAD2 phosphorylation to some extent.

We then tested whether this minimal effective dose of activin B (5 ng/mL) induced hepcidin (*HAMP*) mRNA expression in Hep3B cells and primary mouse hepatocytes. In Hep3B cells, 5-ng/mL activin B significantly increased *HAMP* mRNA up to 50-fold (Figure 1B). Although activin B was less effective than BMP6 to induce *HAMP* mRNA at this low concentration, it had equal potency at higher concentrations (50 ng/mL) (Figure 1C). In contrast, activin A had no significant effect on *HAMP* mRNA expression. The time course of *HAMP* induction was similar for activin B and for BMP6, reaching a peak at 16 hours, and returning to baseline by 24 hours (Figure 1B). In primary mouse hepatocytes, 5-ng/mL activin B also significantly increased *Hamp* mRNA with a similar potency as BMP6, whereas activin A had no significant effect (Figure 1D).

Activin B, but not activin A, induces SMAD1/5/8 phosphorylation with similar potency and kinetics as BMP6 in Hep3B cells and primary mouse hepatocytes

Next, we tested whether the minimal effective dose of activin B (5 ng/mL) induced noncanonical SMAD1/5/8 phosphorylation in Hep3B cells and primary mouse hepatocytes. The potency and kinetics of noncanonical SMAD1/5/8 phosphorylation was compared with canon-

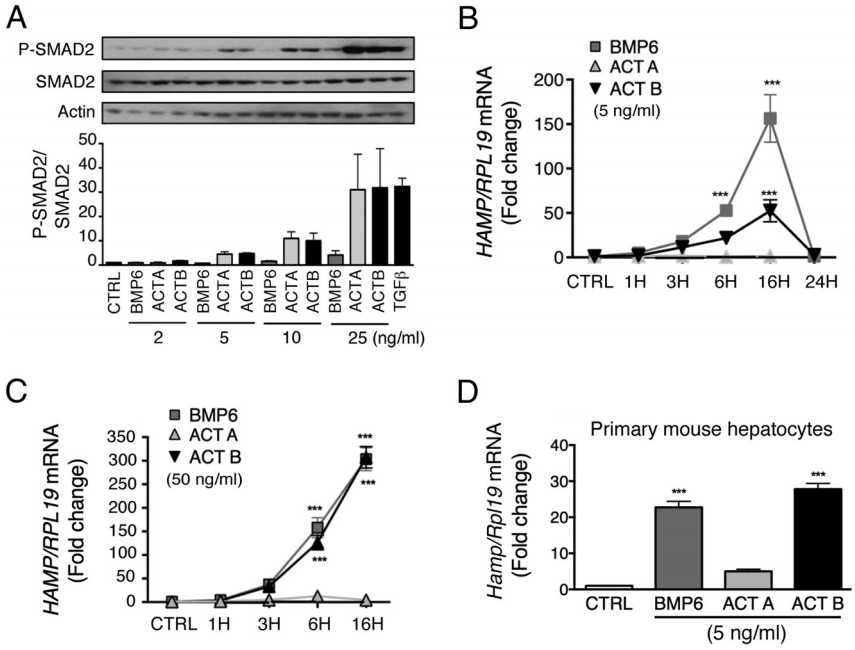

Figure 1. Activin B (ACTB), but not activin A (ACTA), induces hepcidin (*HAMP*) mRNA with similar kinetics and similar or modestly reduced potency compared with BMP6 in Hep3B cells and primary mouse hepatocytes. A, Hep3B cells were treated with the indicated concentrations of BMP6, ACTA, or ACTB or with 0.1-ng/mL TGF-β1 for 6 hours, and cells were analyzed for P-SMAD2 relative to total SMAD2 and actin by immunoblot and chemiluminescence quantification. A representative immunoblot is shown. Chemiluminescence results are reported as mean ± SEM of 3 separate experiments. B–D, Hep3B cells (B and C) and primary mouse hepatocytes (D) were treated without (CTRL) or with 5-ng/mL (B and D) or 50-ng/mL (C) BMP6, ACTA, or ACTB and analyzed at different time points for *HAMP* mRNA expression relative to housekeeping *RPL19* by qRT-PCR. Results are expressed as mean ± SEM of 3 separate experiments each performed in triplicate for the fold change compared with untreated cells at each time point (CTRL), which was normalized to 1. B and C, Statistical significance was determined using two-way ANOVA with Bonferroni post hoc test. For both concentrations, BMP6 and ACTB, but not ACTA, treatment significantly increased *HAMP* mRNA compared with CTRL ($P < .001$). For the 50-ng/mL concentration, BMP6 and ACTB treatment were not significantly different from each other. For the 5-ng/mL concentration, ACTB had a less potent effect than BMP6 ($P < .001$). For each time point, significant changes are shown as ***, $P < .001$ compared with CTRL. D, Statistical significance was determined by one-way ANOVA with Dunnett's post hoc (***, $P < .001$ relative to CTRL).

ical SMAD2/3 phosphorylation, and results were compared with BMP6 and activin A. As shown in Figure 2, activin B stimulated both SMAD1/5/8 phosphorylation and SMAD2/3 phosphorylation in Hep3B cells (Figure 2, A–J) and primary hepatocytes (Figure 2, K–M). Phosphorylation of both SMAD1/5/8 and SMAD2/3 were seen by 1 hour, persisted for 16 hours, and returned to baseline by 24 hours. The degree of SMAD1/5/8 and SMAD2/3 phosphorylation induced by activin B was similar to BMP6 and activin A, respectively; however, neither BMP6 nor activin A crossactivated noncanonical SMAD signaling at low concentrations. Activin B also significantly increased the SMAD1/5/8 target transcript *ID1* mRNA in both cell types (Figure 3). Thus, activin B stimulates noncanonical SMAD1/5/8 signaling and hepcidin expression in hepatocytes to a similar degree as SMAD2/3 signaling, even at low concentrations, with similar kinetics, and with similar or modestly reduced potency compared with BMP6.

Activin B uses SMAD5, but not SMAD2/3, to induce hepcidin in Hep3B cells

Our next focus was to investigate the molecular mechanism by which activin B induces hepcidin. Although a role for noncanonical BMP type I receptors and SMAD1/5/8 in hepcidin induction by activin B was proposed by Besson-Fournier et al (13), their data were inconclusive due to the residual induction of hepcidin by activin B in cells treated with the BMP type I receptor inhibitor LDN-193189 compared with LDN-193189 treatment alone (with a fold increase that appeared similar to the induction of hepcidin by activin B in the absence of LDN-193189). Additionally, the functional importance of canonical type I receptors, which play a key role in noncanonical SMAD crossactivation by other TGF-β superfamily members (28–30, 32–34), canonical SMAD2/3 signaling, type II receptors, and the coreceptor HJV have not been examined. We therefore tested the effects of siRNA knockdown of endogenously expressed canonical and noncanonical R-SMADs, type I receptors, type II receptors, and the coreceptor HJV on activin B stimulation of hepcidin expression in Hep3B cells. As controls, siRNA effects on BMP6 stimulation of hepcidin, as well as activin B or activin A stimulation of canonical SMAD 3 signaling were tested in parallel. Efficacy and specificity of all siRNAs were verified (Supplemental Figures 2–4).

We first explored whether activin B stimulation of hepcidin expression was dependent on canonical SMAD2/3 and/or noncanonical SMAD1/5/8 signaling. SMAD5 siRNA robustly inhibited, whereas SMAD2 and SMAD3 siRNA mildly induced, basal *HAMP* mRNA expression (Figure 4A). Activin B stimulation of *HAMP* mRNA was significantly inhibited by SMAD5, but not SMAD3 or SMAD2 knockdown, similar to BMP6 (Figure 4A). This inhibition was evident even after accounting for reduced basal *HAMP* expression seen with SMAD5 knockdown

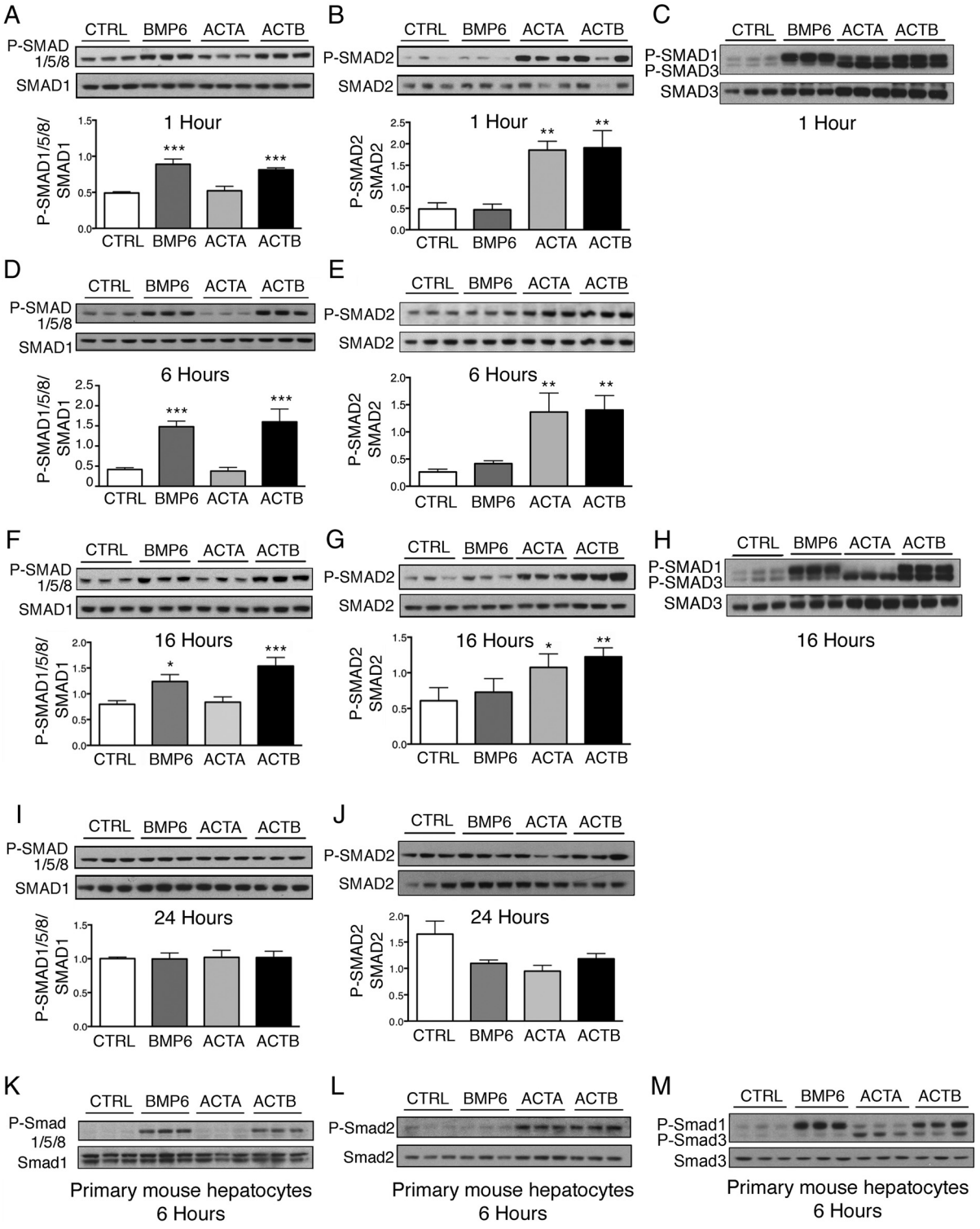

Figure 2. Activin B (ACTB) stimulates SMAD1/5/8 phosphorylation with similar kinetics and potency as BMP6, and SMAD2/3 phosphorylation with similar kinetics and potency as activin A (ACTA) in Hep3B cells and primary mouse hepatocytes. Hep3B cells (A–J) and primary mouse hepatocytes (K–M) were treated without (CTRL) or with 5-ng/mL BMP6, ACTA, or ACTB and analyzed at 1, 6, 16, and 24 hours as indicated for P-SMAD1/5/8 relative to total SMAD1 (A, D, F, I, and K) and for P-SMAD2 relative to total SMAD2 (B, E, G, J, and L) by immunoblot and chemiluminescence quantification. Chemiluminescence results are reported as mean ± SEM of 3 separate experiments (P-SMAD1/5/8) or 2 separate experiment (P-SMAD2) each performed in triplicate. Representative immunoblots are shown. Statistical significance was determined by one-way ANOVA with Dunnett's post hoc test (*, $P < .05$; **, $P < .01$; ***, $P < .001$ relative to CTRL). Activation of the P-SMAD2/3 and P-SMAD1/5/8 pathways was also verified by immunoblot using a P-SMAD3 antibody that recognizes both P-SMAD3 and P-SMAD1 as indicated (C, H, and M). Chemiluminescence quantitation was not performed on primary hepatocyte samples because CTRL bands were too faint, nor on P-SMAD3/1 gels because SMAD3 and SMAD1 bands were too close to each other.

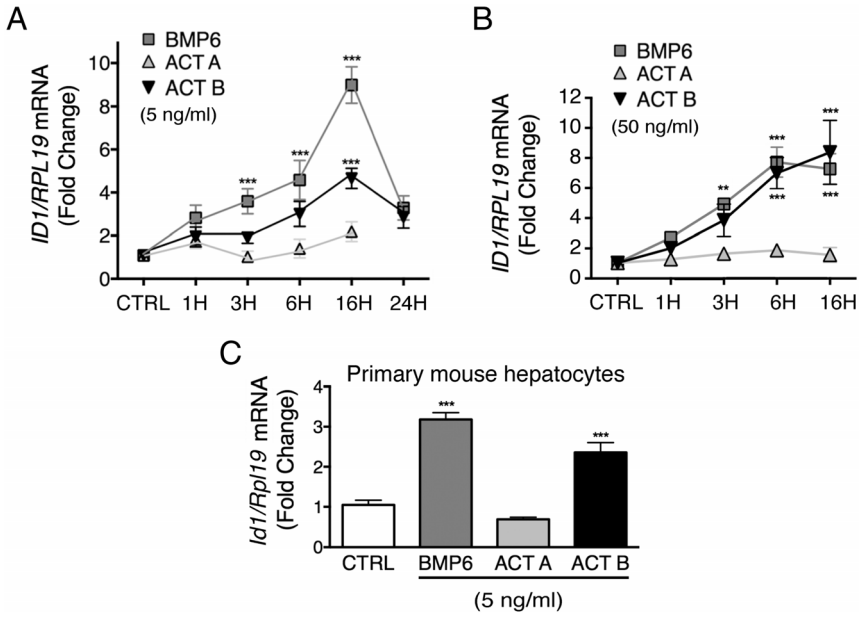

Figure 3. Activin B (ACTB), but not activin A (ACTA), induces *ID1* mRNA with similar kinetics and similar or modestly reduced potency compared with BMP6 in Hep3B cells and primary mouse hepatocytes. Hep3B cells (A and B) and primary mouse hepatocytes (C) treated without (CTRL) or with 5-ng/mL (A and C) or 50-ng/mL (B) BMP6, ACTA, or ACTB for various times as indicated from Figure 1 were analyzed for *ID1* relative *RPL19* mRNA by qRT-PCR. Results are expressed and analyzed as described in Figure 1. A and B, For both concentrations, BMP6 and ACTB, but not ACTA, treatment significantly increased *ID1* mRNA compared with CTRL ($P < .001$). For the 50-ng/mL concentration, BMP6 and ACTB treatment was not significantly different from each other. For the 5-ng/mL concentration, ACTB had a less potent effect than BMP6 ($P < .001$). For each time point, significant changes are shown as **, $P < .01$; ***, $P < .001$ compared with CTRL. C, ***, $P < .001$ relative to CTRL.

(fold induction for activin B treatment relative to unstimulated cells 27 for control siRNA, 6 for SMAD5 siRNA). Results for SMAD3 and SMAD2 knockdown were unchanged after accounting for siRNA effects on basal hepcidin expression. Activin B and BMP6 induction of *ID1* mRNA were similarly inhibited by SMAD5, but not SMAD3 or SMAD2 knockdown (Supplemental Figure 5). In contrast, SMAD3 knockdown inhibited, whereas SMAD5 or SMAD2 knockdown increased, both activin B and activin A stimulation of the SMAD3-specific luciferase reporter CAGA-Luc (Figure 4, B and C). Thus, hepcidin induction by activin B depends on SMAD5 but not SMAD2/3 signaling.

Activin B uses BMP type I receptors ALK2 and ALK3, but not activin type I receptors, to induce hepcidin in Hep3B cells

We then explored whether canonical activin type I receptors (ALK4 and ALK7) and/or BMP type I receptors (ALK2, ALK3, and ALK6) mediate activin B induction of hepcidin. ALK4 and ALK7 siRNA had no effect on basal *HAMP* mRNA (Figure 5A). ALK4 knockdown had no significant effect, whereas ALK7 knockdown increased both activin B and BMP6 stimulation of *HAMP* (Figure 5A) and *ID1* mRNA (Supplemental Figure 6A). In contrast, ALK7 knockdown inhibited activin B, whereas ALK4 knockdown inhibited activin A induction of CAGA-Luc activity (Figure 5, B and C), consistent with reports that activin B preferentially signals via ALK7 compared with activin A, at least in some cellular contexts (47).

When examining BMP type I receptors, ALK6 siRNA had a mild stimulatory effect, whereas ALK2 and ALK3 siRNA had no effect on basal *HAMP* mRNA (Figure 5D). Knockdown of ALK2 and to a lesser extent ALK3 inhibited both activin B and BMP6 induction of *HAMP* and *ID1* mRNA, whereas ALK6 knockdown had no significant effect on *HAMP* or *ID1* mRNA induction by activin B (Figure 5D and Supplemental Figure 6B). Results were unchanged after accounting for the mild stimulatory effect of ALK6 knockdown on basal *HAMP* mRNA expression. Knockdown of each BMP type I receptor increased activin A or activin B induction of CAGA-Luc activity (Figure 5, E and F). These data suggest that although activin B signals via the canonical activin type I receptor ALK7 to stimulate SMAD2/3 signaling, it exclusively uses the BMP type I receptors ALK2 and ALK3 to stimulate SMAD1/5/8 signaling and hepcidin expression in Hep3B cells, similar to BMP6.

Activin B uses canonical type II receptors ACVR2A and ACVR2B to induce hepcidin expression in Hep3B cells

Next, we investigated which type II receptors mediate activin B induction of hepcidin. Activins and BMPs share the type II receptors ACVR2A and ACVR2B. Although BMPR2 is classically described as a type II receptor for BMPs, it can also mediate activin signaling in certain cellular contexts (48). Type II receptor siRNAs had no effect on basal *HAMP* mRNA (Figure 6A). Knockdown of ACVR2A or ACVR2B significantly inhibited activin B induction of both *HAMP* mRNA and CAGA-Luc activity (Figure 6, A and B). In contrast, only ACVR2A knockdown inhibited BMP6 induction of *HAMP* (Figure 6A) and *ID1* mRNA (Supplemental Figure 7), whereas ACVR2B knockdown had the most potent effect on ac-

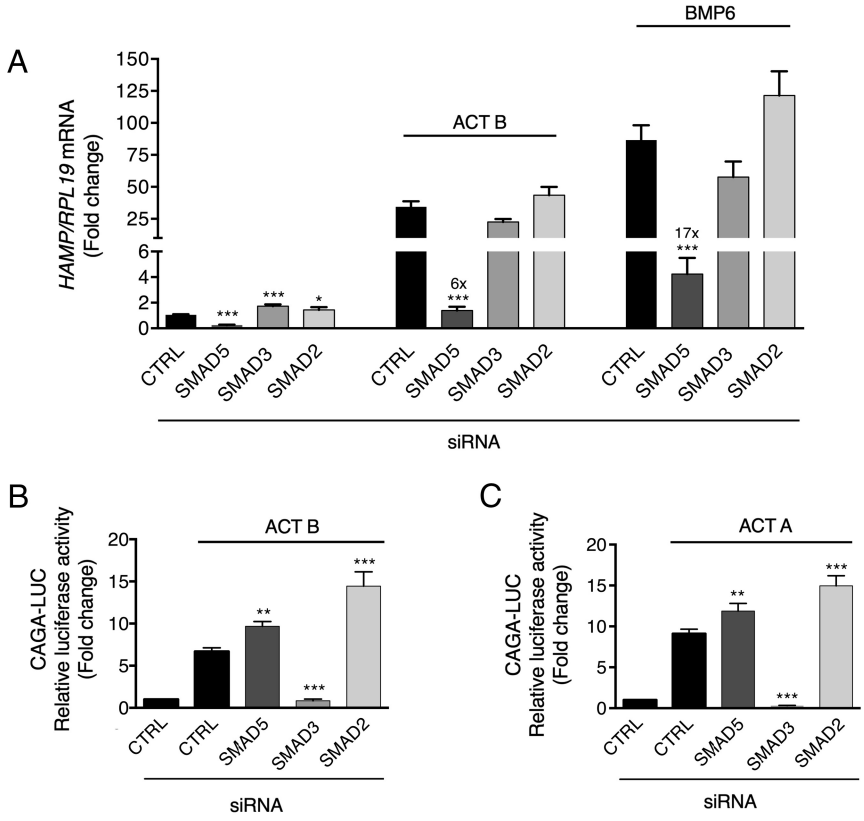

Figure 4. Activin B (ACT B) induction of hepcidin depends on SMAD5, but not SMAD3 or SMAD2, in Hep3B cells. Hep3B cells were transfected with control siRNA (CTRL), siSMAD5, siSMAD3, or siSMAD2 (40nM) either alone (A) or in combination with the SMAD3-responsive firefly luciferase reporter (CAGA-Luc) and pRL-TK control *Renilla* luciferase vector (B and C). Forty-eight hours after transfection, cells were incubated in the absence or presence of 5-ng/mL ACT B, BMP6, or activin A (ACT A) as indicated for 6 hours, followed by measurement of *HAMP* relative to *RPL19* mRNA levels by qRT-PCR (A) or relative luciferase activity (B and C). Data are expressed as the mean ± SEM from 3 separate experiments each performed in triplicate for the fold change relative to untreated control siRNA-transfected cells, which were normalized to 1. Statistical significance was determined by one-way ANOVA compared with control siRNA-transfected cells treated with the same ligand (*, $P < .05$; **, $P < .01$; ***, $P < .001$). For siSMAD5-transfected cells in panel A, fold change relative to untreated siSMAD5-transfected cells is indicated over the respective bars.

tivin A induction of CAGA-Luc activity (Figure 6C). BMPR2 knockdown augmented both BMP6 and activin B effects in this cell line (Figure 6 and Supplemental Figure 7). Thus, activin B uses the same type II receptors, ACVR2A and ACVR2B, to stimulate both canonical and noncanonical R-SMAD signaling and hepcidin expression in Hep3B cells.

Activin B binds directly to HJV and uses HJV to stimulate hepcidin in Hep3B cells

Because the coreceptor HJV plays an important role in BMP6-mediated hepcidin regulation (16, 21), we tested whether HJV affected activin B-mediated hepcidin induction in Hep3B cells. Knockdown of HJV mildly increased basal *HAMP* mRNA but significantly inhibited both activin B and BMP6 induction of *HAMP* mRNA expression (Figure 7A). Conversely, HJV overexpression augmented both activin B and BMP6 stimulation of Hep-Luc (21) activity (Figure 7B). Notably, activin B still retained some ability to induce hepcidin mRNA in primary hepatocytes from *Hjv*−/− mice, albeit to a lesser extent than in WT primary hepatocytes, as previously reported for BMP2 (Figure 7C) (21). Thus, although HJV augments activin B and BMP induction of hepcidin mRNA, it is not required. In contrast, HJV knockdown did not impact activin B stimulated CAGA-Luc activity (Figure 7D). Importantly, activin B was pulled down with protein A beads only in the presence of HJV.Fc (Figure 7E). Moreover, activin B bound directly to HJV with high affinity (K_D, 10.7nM) as measured by SPR (Figure 7F).

Activin B-SMAD1/5/8 signaling exhibits some selectivity for hepatocyte-derived cells and is not enabled by HJV in other cell types

We next explored whether activin B's ability to stimulate SMAD1/5/8 signaling was generalizable to other cell types. We hypothesized that the presence of HJV (also known as repulsive guidance molecule [RGM]C) or the homologous BMP coreceptors RGMA or RGMB might be important to facilitate the formation of receptor complexes favorable to activin B-SMAD1/5/8 signaling. We therefore compared cell lines that express endogenous RGMs (Hep3B and C2C12 cells) with those that do not (KGN and IMCD cells) (Supplemental Figure 8A). Although activin B stimulated activity of the BMP-SMAD1/5/8-responsive luciferase reporter (BRE-Luc) (39) in Hep3B cells, it did not significantly affect BRE-Luc activity in other cell lines tested (Figure 7G), even at concentrations up to 50 ng/mL (data not shown). In contrast, BMP6 stimulated BRE-Luc activity (Figure 7G), and activin B or A stimulated CAGA-Luc activity or SMAD2 phosphorylation in all cell lines tested (Supplemental Figure 8, B and C). In IMCD cells that lack endogenous RGMs, whereas HJV transfection increased

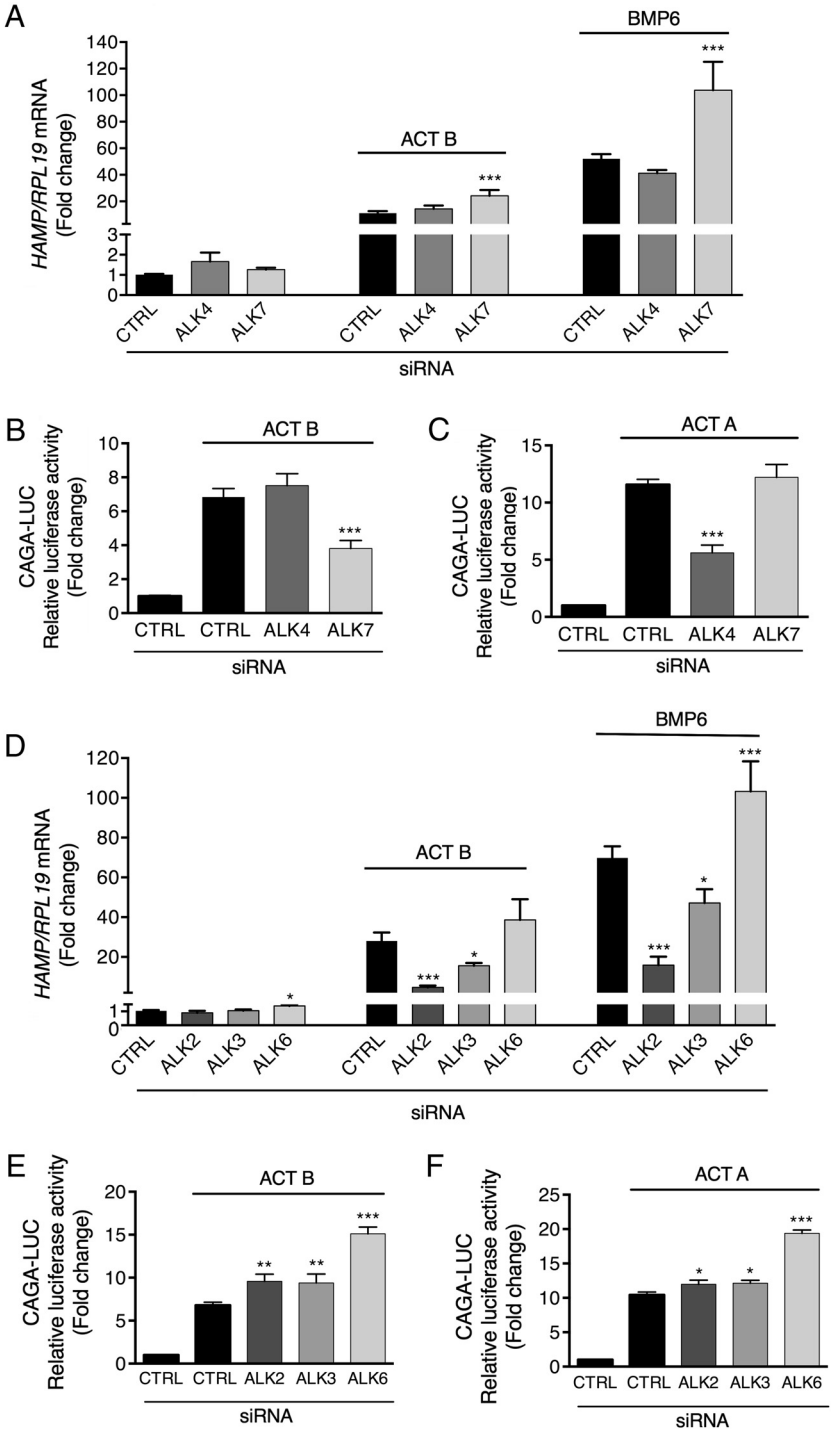

Figure 5. Activin B (ACT B) uses the activin type I receptor ALK7 to stimulate SMAD3 signaling but the BMP type I receptors ALK2 and ALK3 to stimulate hepcidin in Hep3B cells. Hep3B cells were transfected with control siRNA (CTRL), siALK4, siALK7, siAKL2, siALK3, or siALK6 (40nM) either alone (A and D) or in combination with CAGA-Luc and pRL-TK (B, C, E, and F). Forty-eight hours after transfection, cells were incubated in the absence or presence of 5-ng/mL ACT B, BMP6, or activin A (ACT A) as indicated for 6 hours, followed by measurement of *HAMP* relative to *RPL19* mRNA levels by qRT-PCR (A and D) or relative luciferase activity (B, C, E, and F). Data are expressed and analyzed as described in Figure 4.

basal and BMP6-stimulated BRE-Luc activity, it had no impact on activin B stimulation of BRE-Luc activity (Figure 7H).

Liver activin B is up-regulated in multiple mouse models of inflammation associated with elevated hepcidin levels

Finally, we investigated whether activin B has a physiologic role in hepcidin induction by inflammation in vivo. We found that liver activin B (*Inhbb*) mRNA was up-regulated in multiple mouse models of inflammation associated with increased hepcidin levels and hypoferremia including LPS, turpentine, and BA models (Figure 8 and Supplemental Figure 9). *Inhbb* mRNA levels peaked at 6 hours after induction in acute inflammatory models and persisted for up to 11 days in the chronic BA model (Figure 8, A–C). Interestingly, although acute inflammation and in particular TNFα were previously associated with robust down-regulation of liver *Hjv* mRNA (49), which we confirmed in our LPS and BA models (Supplemental Figure 9, D and F), Hjv protein expression was more modestly affected with no change 4 hours after LPS, approximately 35%–40% reduction 6 hours after LPS or BA (Figure 8, G and I), and no change in the turpentine model (Figure 8H), where *Hjv* mRNA was also not reduced (Supplemental Figure 9E). *Hjv* mRNA expression increased back to approximately 60% of baseline levels in the chronic BA model (Supplemental Figure 9F).

FST315 has no impact on basal hepcidin or iron parameters but inhibits hepcidin induction by inflammation in mice

We then tested whether injection of FST315, a secreted protein that binds and inhibits activin activity (51), impacted hepcidin up-regulation by LPS and BA in mice. FST315 caused a dose-dependent inhibition of activin B-stimulated Hep-Luc and CAGA-Luc activity in Hep3B cells but did not affect BMP6 signaling at doses up to 400 μg/mL (Figure 9A and data not shown). FST315

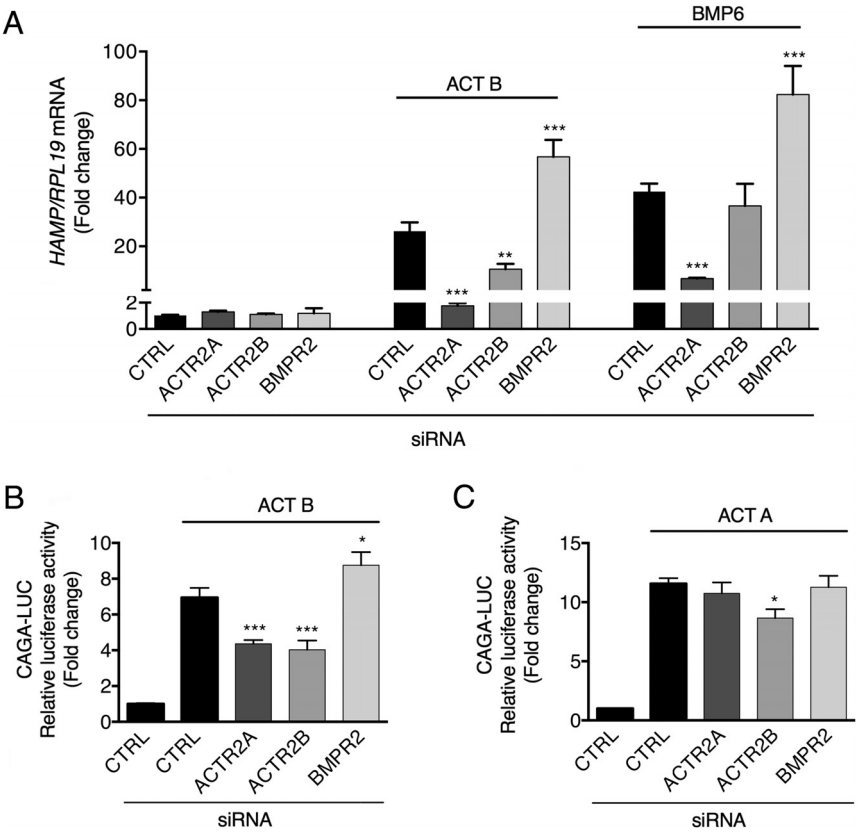

Figure 6. Activin B (ACT B) uses the type II receptors ACVR2A and ACVR2B to stimulate both SMAD3 signaling and hepcidin in Hep3B cells. Hep3B cells were transfected with control siRNA (CTRL), siBMPR2, siACVR2A, or siACVR2B (40nM), either alone (A) or in combination with CAGA-Luc and pRL-TK (B and C). Forty-eight hours after transfection, cells were incubated in the absence or presence of 5-ng/mL ACT B, BMP6, or activin A (ACT A) as indicated for 6 hours, followed by measurement of *HAMP* relative to *RPL19* mRNA levels by qRT-PCR (A) or relative luciferase activity (B and C). Data are expressed and analyzed as described in Figure 4.

injection alone in mice did not significantly impact liver *Hamp* or *Id1* mRNA expression or serum iron parameters (Figure 9, B–D). However, FST315 significantly inhibited liver *Hamp* mRNA induction by LPS (Figure 9E). Whereas FST315 treatment did not affect induction of liver *Il6* mRNA and phosphorylated Stat3 protein by LPS (Figure 9, F and G), liver P-Smad5 induction was significantly inhibited (Figure 9H), and *Id1* mRNA induction was blunted (Figure 9I). Despite inhibiting *Hamp* mRNA expression, FST315 did not significantly reverse the hypoferremia induced by LPS at 6 hours (Figure 9J). Of note, duodenum divalent metal transporter 1 (*Dmt1*) and duodenum and spleen ferroportin (*Fpn*) mRNA were robustly inhibited by LPS treatment (Figure 9K), similar to previous reports (52, 53), suggesting that other hepcidin-independent mechanisms may contribute hypoferremia in the early inflammatory response. The ability of FST315 to blunt liver *Hamp* mRNA induction was also demonstrated in the BA model at 6 hours (Figure 9L).

Discussion

Anemia is a common complication of chronic inflammatory conditions and is associated with poorer outcomes and a lower quality of life (1). High hepcidin contributes to the anemia of inflammation by restricting iron availability (1). Here, we provide the first experimental evidence suggesting that activin B has a functional role in hepcidin induction by inflammation in vivo by showing that administration of the activin inhibitor FST315 blunts hepcidin induction by LPS and BA.

Although follistatin was previously reported to alter cytokine stimulation by LPS and to improve survival after a lethal LPS injection by inhibiting activin A (54), we did not see any effect of FST315 on LPS- or BA-induced liver *Il6* mRNA expression or Stat3 phosphorylation. Thus, the hepcidin lowering effects of FST315 in our models were not due to inhibition of the liver IL-6-STAT3 pathway. Instead, our data suggest that FST315 inhibited hepcidin by reducing liver Smad5 phosphorylation. These data are consistent with previous studies showing that other SMAD1/5/8 signaling inhibitors also blunted hepcidin induction by inflammatory stimuli without impacting the STAT3 phosphorylation (10, 11). These data reinforce the notion that a functional SMAD1/5/8 pathway is required for the STAT3 pathway to maximally induce hepcidin.

A limiting factor of our in vivo study is that FST315 is not specific for activin B but also binds other TGF-β superfamily members, including activin A, myostatin/growth and differentiation factor (GDF)8, GDF11, BMP6, and BMP7 (35, 51). Of note, follistatin has a lower binding affinity for BMPs and GDFs compared with activins (35, 51). Moreover, FST315 is much less potent to inhibit the biological activity of BMP6 and BMP7 compared with activins (51), which is also corroborated by our in vitro data. Importantly, whereas a neutralizing BMP6 antibody inhibited basal hepcidin expression and increased serum iron in mice (16), FST315 had no effect on basal hepcidin expression or serum iron parameters in our study. Instead, FST315 only inhibited hepcidin in the context of an inflammatory stimulus when liver activin B

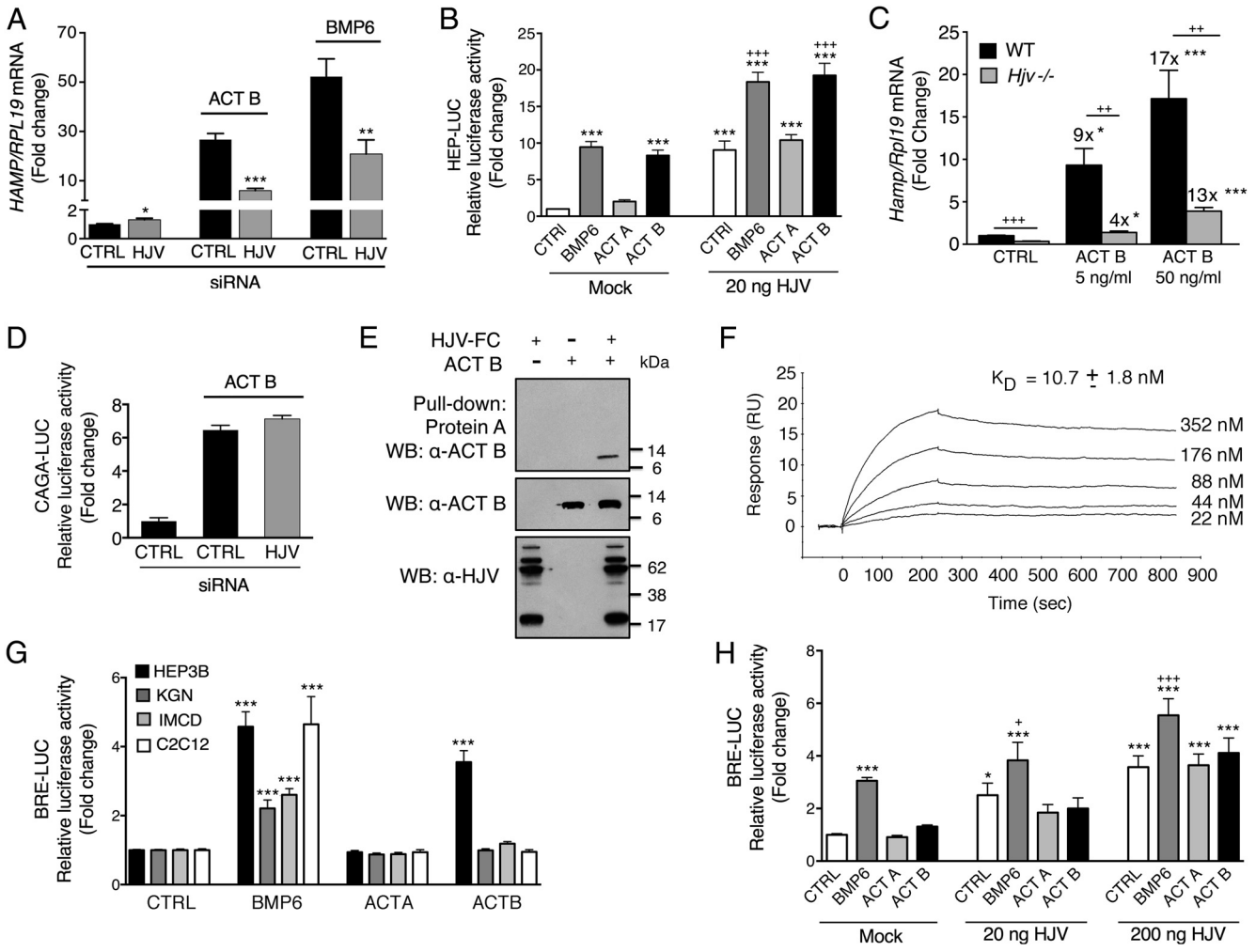

Figure 7. Activin B (Act B) interacts with the coreceptor HJV to stimulate hepcidin expression in Hep3B cells, but the presence of HJV is not sufficient to enable activin B-SMAD1/5/8 signaling in nonhepatocyte cells. A and D, Hep3B cells were transfected with control siRNA (CTRL) or siHJV (40nM) without (A) or with CAGA-Luc and pRL-TK (D). Forty-eight hours after transfection, cells were incubated in the absence or presence of 5-ng/mL Act B or BMP6 as indicated followed by measurement of *HAMP* relative to *RPL19* mRNA levels by qRT-PCR (A) or relative luciferase activity (D). Data are expressed as the mean ± SEM from 3 separate experiments each performed in triplicate for the fold change relative to untreated control siRNA-transfected cells, which were normalized to 1. Statistical significance was determined by 2-tailed Student's *t* test for siHJV compared with siCTRL-transfected cells for each treatment condition (*, $P < .05$; **, $P < .01$; ***, $P < .001$). B and H, Hep3B cells (B) or IMCD cells (H) were transfected with Hep-Luc (B) or BRE-Luc (H) and pRL-TK, in combination with empty vector (mock) or the indicated concentrations of cDNA encoding HJV. Forty-eight hours after transfection, cells were treated in the absence (CTRL) or presence of 5-ng/mL BMP6, activin A (Act A), or Act B for 6 hours, followed by measurement of relative luciferase activity. Data are expressed as the mean ± SEM from 2 (H) or 3 (B) separate experiments each performed in triplicate for the fold change relative to mock-transfected untreated cells, which was normalized to 1. Statistical significance was determined by one-way ANOVA with Tukey post hoc test (*, $P < .05$; ***, $P < .001$ relative to untreated mock-transfected cells; and +, $P < .05$; +++, $P < .001$ relative to untreated HJV-transfected cells at each concentration). C, Primary hepatocytes isolated from *Hjv*−/− or littermate WT control mice were incubated in the absence or presence of 5- or 50-ng/mL Act B followed by measurement of *Hamp* relative to *Rpl19* mRNA by qRT-PCR. Results are expressed as mean ± SEM from 4 separate experiments each performed in duplicate or triplicate for the fold change compared with untreated WT primary hepatocytes, which was normalized to 1. For *Hjv*−/− hepatocytes, fold change compared with untreated *Hjv*−/− hepatocytes is indicated above the relevant columns. Statistical significance was determined by one-way ANOVA with Dunnett's post hoc test compared with untreated cells for each genotype (*, $P < .05$; **, $P < .01$,***, $P < .001$), and by 2-tailed Student's *t* test for *Hjv*−/− compared with WT cells for each ligand concentration (++, $P < .01$; +++, $P < .001$). E, Purified Act B alone, HJV.Fc alone, or Act B in combination with HJV.Fc was incubated in solution. Act B bound to HJV.Fc was precipitated with protein A beads, and the eluted protein complex was analyzed by SDS-PAGE, followed by immunoblot with activin B antibody (α-Act B) under reducing conditions (upper panel). As a control to demonstrate input proteins, solution aliquots before Protein-A pull-down were also analyzed by immunoblot with anti-HJV antibody (α-HJV) and α-Act B under reducing conditions (lower panels). Representative immunoblots from 1 of 3 separate experiments is shown. F, HJV protein was diluted in running buffer HBS-EP+ into a series of concentrations (22nM, 44nM, 88nM, 176nM, and 352nM) and injected through a CM5 chip immobilized with Act B at 1000 RU. Binding affinity (K_D) was measured by SPR. A representative sensogram is shown. The mean K_D ± SEM from 3 separate experiments is reported. G, Hep3B, IMCD, C2C12, and KGN cells were transfected with BRE-Luc and pRL-TK. Forty-eight hours after transfection, cells were treated with 5-ng/mL BMP6, Act B, or Act A for 6 hours, followed by measurement of relative luciferase activity. Data are expressed as the mean ± SEM from 3 separate experiments each performed in triplicate for the fold change relative to untreated cells, which were normalized to 1. Statistical significance was determined by one-way ANOVA with Dunnett's post hoc test (***, $P < .001$ relative to untreated cells).

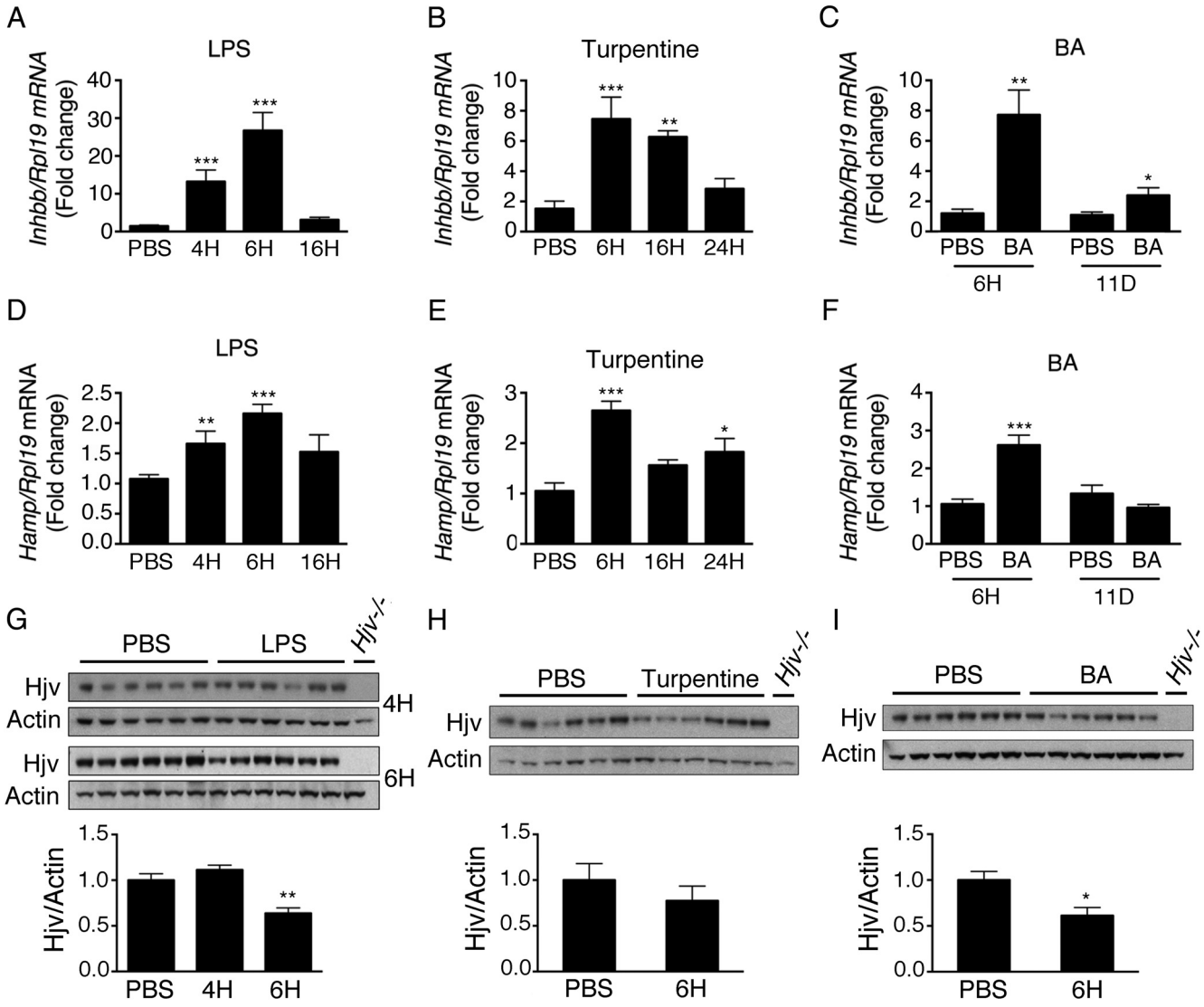

Figure 8. Liver activin B mRNA expression is up-regulated in multiple mouse models of inflammation associated with increased hepcidin. A, D, and G, Eight-week-old C57BL/6 male mice received an ip injection of LPS in or an equal volume of PBS alone. Mice were analyzed 4, 6, or 16 hours after injection (n = 6–12 mice per group). B, E, and H, Eight-week-old C57BL/6 male mice received a sc intrascapular injection of oil of turpentine or an equal volume of PBS alone. Mice were analyzed at 6, 16, or 24 hours after injection (n = 5–6 mice per group). C, F, and I, Eight-week-old C57BL/6 male mice received an ip injection of heat-killed BA or an equal volume of PBS alone. Mice were analyzed 6 hours or 11 days after injection (n = 6 mice per group). Total liver RNA was analyzed by qRT-PCR for activin B (*Inhbb*) (A–C) and *Hamp* relative to *Rpl19* mRNA (D–F), with results reported as mean ± SEM for the fold change relative to the PBS group, which was normalized to 1. Phosphatidylinositol phospholipase C treated liver protein extracts from the indicated groups were analyzed for Hjv relative to actin protein expression by immunoblot and chemiluminescence quantification (G–I). Immunoblots show the dominant 35-kDa band seen by this technique (50). Liver tissue from *Hjv*−/− mice was used as a negative control. Statistical significance was determined by Student's *t* test (C, F, H, and I) or one-way ANOVA with Dunnett's post hoc test with *, $P < .05$; **, $P < .01$; ***, $P < .001$ relative to the control (PBS) group.

mRNA expression was increased. These data suggest that FST315 does not inhibit BMP6 at the doses used in our study and that activins do not contribute to basal hepcidin expression or iron homeostasis. Although our in vivo data cannot rule out a role for other ligands in hepcidin induction by inflammation, our in vitro data demonstrate that activin B, but not activin A, potently crossactivates noncanonical SMAD1/5/8 signaling to induce hepcidin expression in hepatocytes. We therefore hypothesize that inhibiting activin B is likely the mechanism by which FST315 inhibits SMAD1/5/8 signaling and hepcidin induced by LPS. Future studies will be needed to confirm this hypothesis in vivo with more specific activin B inhibitors.

Although crossactivation of noncanonical SMAD signaling has been reported for other TGF-β superfamily ligands in certain cellular contexts (28–34), activin B stimulation of SMAD1/5/8 signaling in liver cells is unique in many ways. First, activin B was similarly potent to stimulate noncanonical SMAD1/5/8 and canonical SMAD2/3 signaling at low concentrations. This contrasts with other

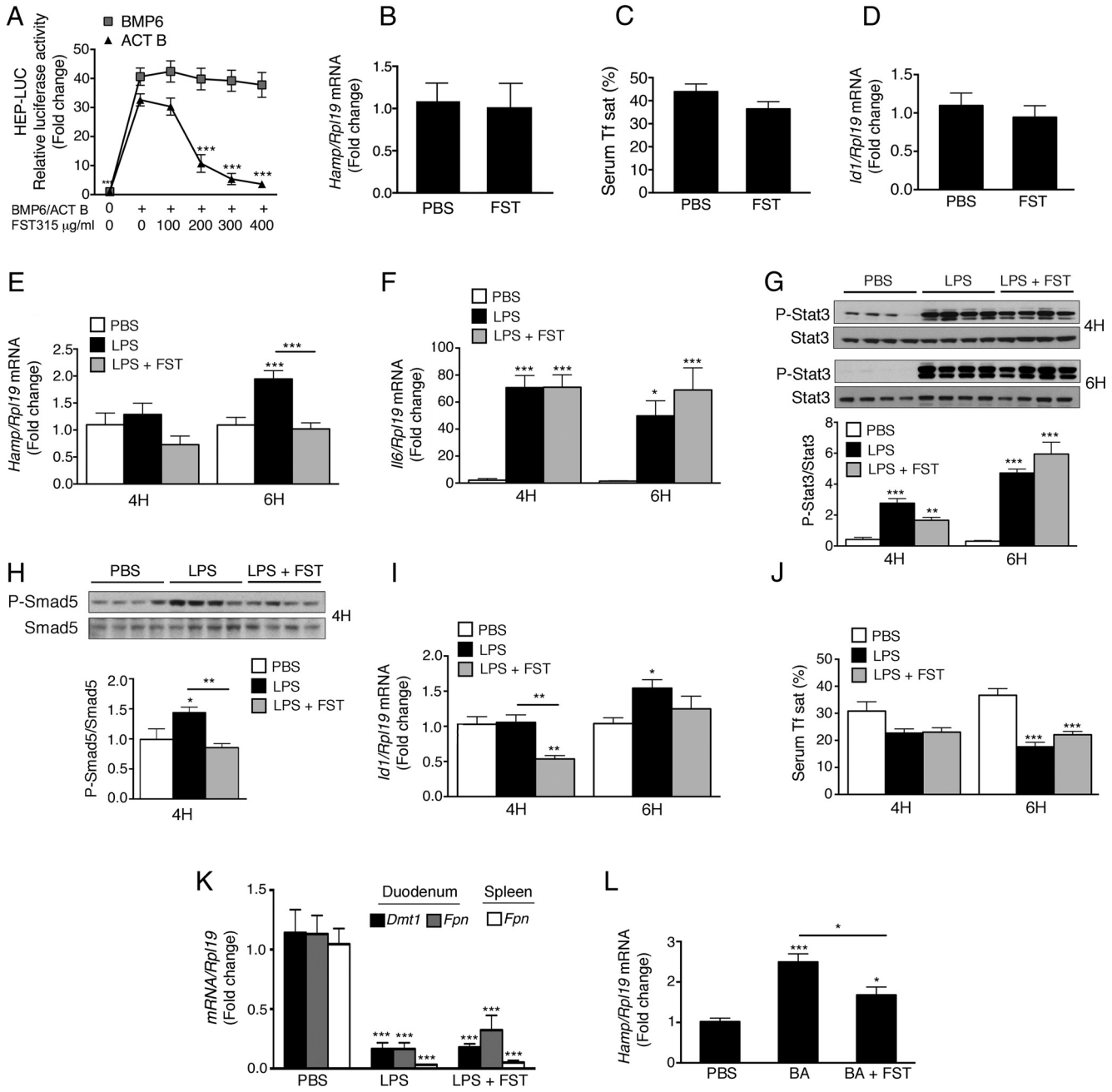

Figure 9. Inhibition of activin B by FST315 administration has no effect on basal hepcidin expression but blunts hepcidin induction by LPS and BA in mice. A, Hep3B cells were transfected with Hep-Luc and pRL-TK. Forty-eight hours after transfection, cells were incubated in the absence or presence 50-ng/mL Act B or BMP6 for 16 hours, without or with cotreatment with increasing concentrations of FST315, followed by measurement of relative luciferase activity. Results are reported as the mean ± SEM from 2 separate experiments each performed in triplicate for the fold change relative to BMP6/Act B-treated cells without FST315. Statistical significance was determined by two-way ANOVA with Dunnett's post hoc test; ***, $P < .001$ relative to BMP6/Act B-treated cells without FST315. B–L, Eight-week-old C57BL/6 male mice received an ip injection of 50-μg FST315 in PBS or PBS alone (B–D). Alternatively, mice received an ip injection of LPS (E–K), BA (L), or an equal volume of PBS alone, together with a second injection of PBS alone or 50-μg FST315 in PBS. Mice were analyzed 4 or 6 hours after injection (n = 11–12 mice per group in a total of 2 independent experiments for the 6-h LPS group; n = 6 mice per group for all other experiments). Total liver RNA was analyzed by qRT-PCR for *Hamp* (B, E and L), IL-6 (*Il6*) (F), and *Id1* (D and I) relative to *Rpl19* mRNA, with results reported as mean ± SEM for the fold change relative to the PBS group, which was normalized to 1. Liver protein extracts from a subset of mice (n = 6 per group) were analyzed for phosphorylated Stat-3 (P-Stat3) relative to total Stat-3 (G) or phosphorylated Smad5 (P-Smad5) relative to total Smad5 (H) by immunoblot and chemiluminescence quantification. Representative immunoblots are shown. Serum was analyzed for transferrin saturation (Tf sat) (C and J). Total duodenum and spleen RNA was analyzed by qRT-PCR for *Dmt1* and *Fpn* relative to *Rpl19* mRNA, with results reported as mean ± SEM for the fold change relative to the PBS group (K). B–D, Statistical significance was determined by 2-tailed Student's *t* test. E–L, Statistical significance was determined for each time point by one-way ANOVA with Tukey post hoc test (*, $P < .05$; **, $P < .01$; ***, $P < .001$ relative to the control (PBS) group or as otherwise indicated).

reports of noncanonical SMAD signaling, which typically occurred only at higher ligand concentrations (28–31). Second, the 16-hour duration of SMAD1/5/8 activation by activin B was similar to activation of canonical SMAD pathways by activin B and BMP6. In contrast, noncanonical SMAD signaling in previous reports was much more transient, on the order of 1–2 hours (28–32).

A third unique feature is the mechanism of noncanonical SMAD signaling by activin B. The classical understanding is that the specificity of the SMAD signaling response is determined by the L45 loop in the type I receptor kinase domain, which interacts with the L3 loop in the R-SMAD MH2 domain (55). The L45 sequences of the activin and TGF-β type I receptors ALKs 4, 5, and 7 are identical and preferentially activate SMAD2/3, whereas BMP type I receptors are composed of 2 subgroups (ALK3/6 and ALK1/2) whose L45 sequences are different and preferentially activate SMAD1/5/8 (33, 55). However, ALK5 and ALK3 have been shown crossactivate noncanonical SMADs under some conditions (32, 33). TGF-β and BMP2 can also stimulate noncanonical SMAD signaling via heteromeric complexes containing both canonical and noncanonical type I receptors in certain cellular contexts (28–30, 32–34). The requirement of higher ligand concentrations and shorter duration of noncanonical SMAD activation in these studies may reflect a less stable heteromeric receptor complex and/or weaker activation of noncanonical SMADs by type I receptors. In contrast, our data suggests that in hepatocytes, activin B signals via its canonical type II receptors, in combination with BMP type I receptors and the coreceptor HJV, to activate SMAD1/5/8 signaling and hepcidin expression (Figure 10). In our model, the mechanism of crossactivation occurs at the level of type I receptor recruitment. Because this model uses a standard type II/type I receptor complex and canonical type I receptor-SMAD activation pathway, this may explain why activin B-SMAD1/5/8 signaling has a similar dose response and kinetics compared with canonical activin B and BMP6 signaling.

Interestingly, activin B's ability to stimulate SMAD1/5/8 signaling was not universal but exhibited some selectivity to hepatocyte-derived cells. This could explain why noncanonical SMAD1/5/8 signaling by activin B was not previously recognized. Moreover, this is consistent with the cell context-specific nature of noncanonical SMAD signaling reported for other TGF-β superfamily ligands (28–34). Why some cells exhibit noncanonical SMAD signaling and others do not is still poorly understood, al-

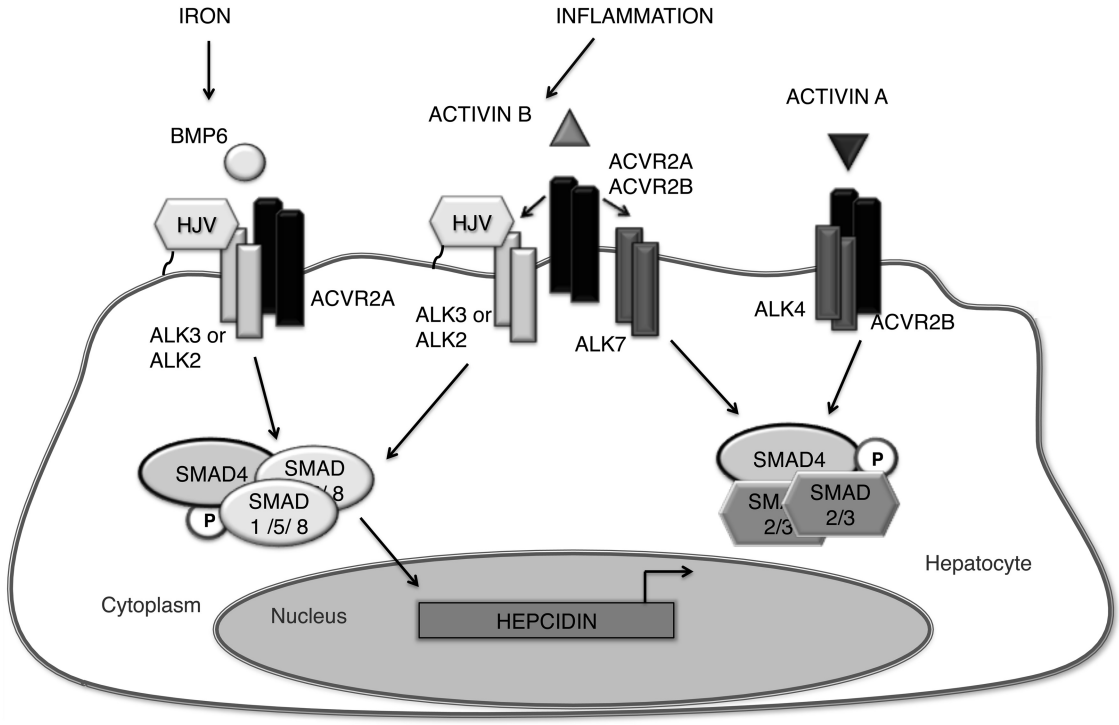

Figure 10. Proposed model for activin B-mediated hepcidin regulation in hepatocytes. Under inflammatory conditions, activin B expression is stimulated in the liver and binds to its canonical type II receptors ACVR2A and ACVR2B, which can recruit either its canonical type I receptor ALK7 to stimulate SMAD2/3 phosphorylation or noncanonical BMP type I receptors ALK2 and ALK3 and the coreceptor HJV to stimulate SMAD1/5/8 phosphorylation. Iron regulates SMAD1/5/8 phosphorylation through BMP6, which activates a similar receptor complex that differs only in type II receptor utilization. Phosphorylated SMAD1/5/8 stimulated by activin B or BMP6 complexes with common mediator SMAD4 to stimulate hepcidin transcription. Activin A signals in hepatocytes via ACVR2B and ALK4 to stimulate SMAD2/3 phosphorylation, which does not stimulate hepcidin expression.

though receptor expression levels have been proposed to contribute (28, 31). In our study, although the coreceptor HJV bound to activin B and enhanced activin B-hepcidin signaling in hepatocyte-derived cells, the presence of HJV or other RGMs was not sufficient to enable activin B-SMAD1/5/8 signaling in other cell types. Interestingly, we often observed a stimulation of one TGF-β superfamily pathway branch, when members of another branch were knocked down. For example, knockdown of ALK7 or BMPR2 induced both activin B- and BMP6-SMAD1/5/8 signaling. We hypothesize that inhibition of ALK7 or BMPR2 increased the formation of receptor complexes favorable to activin B- and BMP6-SMAD1/5/8 signaling (ie, containing ACVR2A and ALK2 or ALK3). Relative expression levels of these receptors could be one factor facilitating activin B-SMAD1/5/8 signaling in hepatocytes, and/or there may be some other accessory protein that is important to enable activin B-SMAD1/5/8 signaling in these cells. Future experiments are needed to understand whether activin B-SMAD1/5/8 signaling is truly unique to hepatocyte-derived cells, to determine the underlying characteristic of these cells that enables activin B-SMAD1/5/8 signaling, to elucidate why activin A with 65% sequence homology to activin B does not share its noncanonical SMAD1/5/8 signaling ability, and to establish whether activin B-SMAD1/5/8 signaling has functional roles other than hepcidin regulation under inflammatory conditions.

HJV was not only insufficient to enable activin B-SMAD1/5/8 signaling nonresponsive cells, it was also not required for activin B-SMAD1/5/8 signaling in hepatocyte-derived cells, because activin B still induced hepcidin expression in *Hjv*−/− primary hepatocytes, albeit to a lesser extent that WT primary hepatocytes. This may explain why LPS still induced hepcidin in *Hjv*−/− mice, although the maximal hepcidin expression achieved was less than in WT mice (22). These data are consistent with previous reports that although HJV and other RGM family coreceptors enhance cellular response to BMP ligands, they are not required for BMP signaling (21). Notably, although *Hjv* mRNA is robustly inhibited by LPS and other acute inflammatory stimuli via TNFα (49), Hjv protein expression was not changed at 4 hours and was more modestly reduced at 6 hours. Thus, HJV protein is present to contribute to activin B regulation of hepcidin expression in these settings. Moreover, *Hjv* expression was more modestly reduced in chronic inflammatory conditions (eg, BA 11 d). We hypothesize that modulation of HJV expression could be one mechanism by which activin B regulation of hepcidin expression is fine-tuned in the context of inflammation.

Interestingly, although FST315 inhibited hepcidin induction by inflammation in the acute LPS and BA models, hypoferremia was not reversed by FST315 treatment in these models. This is consistent with 2 previous reports (52, 53), suggesting that hypoferremia in the early inflammatory response is not entirely hepcidin dependent. For example, hypoferremia still occurred in *Hamp*+/− mice where *Hamp* expression was not increased by LPS (similar to our FST315-treated animals), and to a lesser extent in *Hamp*−/− mice (52). Moreover, hypoferremia was induced by the toll-like receptor 2/6 activator FSL1 (a lipoprotein ligand from *Mycoplasma salivarium*), in the absence of hepcidin stimulation (53). Other hepcidin-independent mechanisms proposed to contribute to hypoferremia in this context include the down-regulation of duodenum and spleen Dmt1, duodenum cytochrome b, and duodenum, spleen, and liver ferroportin at the mRNA level (52, 53). We found a similar robust inhibitory effect of LPS on *Dmt1* and *Fpn* mRNA expression in our study.

Despite a lack of FST315 impact on hypoferremia in the acute setting, our data provide proof of concept that activin inhibitors can functionally inhibit hepcidin in the context of inflammation. Inhibiting hepcidin was previously demonstrated to improve iron availability and hemoglobin levels in more chronic animal models of anemia of inflammation (1, 10, 11). Interestingly, one class of hepcidin inhibitors with proven efficacy to treat anemia of inflammation were thought to function by blocking BMP signaling, including soluble HJV and BMP type I receptor inhibitors (10, 11). Our data raise the possibility that one mechanism of action of these agents may be to inhibit activin B stimulation of hepcidin expression, because activin B binds to HJV and uses BMP type I receptors to induce hepcidin. Future studies will be needed to test whether FST315 and/or other more specific activin B inhibitors can also reverse hypoferremia and anemia in chronic inflammatory models. Understanding the detailed molecular mechanisms of the activin B-hepcidin signaling pathway may lead to the development of more targeted treatments for anemia of inflammation.

Acknowledgments

We thank Henry T. Keutmann for technical assistance with production of follistatin-315.

Corresponding author and person to whom reprint requests should be addressed: Jodie L. Babitt, MD, Massachusetts General Hospital, 185 Cambridge Street, CPZN-8208, Boston, MA 02114. E-mail: babitt.jodie@mgh.harvard.edu.

This work was supported in part by National Institutes of Health grant RO1-DK087727 and a Howard Goodman Fellow-

ship Award from the Massachusetts General Hospital to J.L.B. and by NIH NRSA training grant T32 DK007540 to A.B.C.

Disclosure Summary: J.L.B. has ownership interest in Ferrumax Pharmaceuticals, which has licensed technology from the Massachusetts General Hospital based on work cited here and in prior publications. All other authors have nothing to disclose.

References

1. **Sun CC, Vaja V, Babitt JL, Lin HY.** Targeting the hepcidin-ferroportin axis to develop new treatment strategies for anemia of chronic disease and anemia of inflammation. *Am J Hematol*. 2012;87(4):392–400.
2. **Ganz T.** Systemic iron homeostasis. *Physiol Rev*. 2013;93(4):1721–1741.
3. **Wrighting DM, Andrews NC.** Interleukin-6 induces hepcidin expression through STAT3. *Blood*. 2006;108(9):3204–3209.
4. **Pietrangelo A, Dierssen U, Valli L, et al.** STAT3 is required for IL-6-gp130-dependent activation of hepcidin *in vivo*. *Gastroenterology*. 2007;132(1):294–300.
5. **Verga Falzacappa MV, Vujic Spasic M, Kessler R, Stolte J, Hentze MW, Muckenthaler MU.** STAT3 mediates hepatic hepcidin expression and its inflammatory stimulation. *Blood*. 2007;109(1):353–358.
6. **Core AB, Canali S, Babitt JL.** Hemojuvelin and bone morphogenetic protein (BMP) signaling in iron homeostasis. *Front Pharmacol*. 2014;5:104.
7. **Wang RH, Li C, Xu X, et al.** A role of SMAD4 in iron metabolism through the positive regulation of hepcidin expression. *Cell Metab*. 2005;2(6):399–409.
8. **Mayeur C, Lohmeyer LK, Leyton P, et al.** The type I BMP receptor Alk3 is required for the induction of hepatic hepcidin gene expression by interleukin-6. *Blood*. 2014;123(14):2261–2268.
9. **Babitt JL, Huang FW, Xia Y, Sidis Y, Andrews NC, Lin HY.** Modulation of bone morphogenetic protein signaling in vivo regulates systemic iron balance. *J Clin Invest*. 2007;117(7):1933–1939.
10. **Theurl I, Schroll A, Sonnweber T, et al.** Pharmacologic inhibition of hepcidin expression reverses anemia of chronic inflammation in rats. *Blood*. 2011;118(18):4977–4984.
11. **Steinbicker AU, Sachidanandan C, Vonner AJ, et al.** Inhibition of bone morphogenetic protein signaling attenuates anemia associated with inflammation. *Blood*. 2011;117(18):4915–4923.
12. **Verga Falzacappa MV, Casanovas G, Hentze MW, Muckenthaler MU.** A bone morphogenetic protein (BMP)-responsive element in the hepcidin promoter controls HFE2-mediated hepatic hepcidin expression and its response to IL-6 in cultured cells. *J Mol Med (Berl)*. 2008;86(5):531–540.
13. **Besson-Fournier C, Latour C, Kautz L, et al.** Induction of activin B by inflammatory stimuli up-regulates expression of the iron-regulatory peptide hepcidin through Smad1/5/8 signaling. *Blood*. 2012;120(2):431–439.
14. **Miyazono K, Kamiya Y, Morikawa M.** Bone morphogenetic protein receptors and signal transduction. *J Biochem*. 2010;147(1):35–51.
15. **Corradini E, Babitt JL, Lin HY.** The RGM/DRAGON family of BMP co-receptors. *Cytokine Growth Factor Rev*. 2009;20(5–6):389–398.
16. **Andriopoulos B Jr, Corradini E, Xia Y, et al.** BMP6 is a key endogenous regulator of hepcidin expression and iron metabolism. *Nat Genet*. 2009;41(4):482–487.
17. **Meynard D, Kautz L, Darnaud V, Canonne-Hergaux F, Coppin H, Roth MP.** Lack of the bone morphogenetic protein BMP6 induces massive iron overload. *Nat Genet*. 2009;41(4):478–481.
18. **Mayeur C, Leyton PA, Kolodziej SA, Yu B, Bloch KD.** BMP type II receptors have redundant roles in the regulation of hepatic hepcidin gene expression and iron metabolism. *Blood*. 2014;124(13):2116–2123.
19. **Steinbicker AU, Bartnikas TB, Lohmeyer LK, et al.** Perturbation of hepcidin expression by BMP type I receptor deletion induces iron overload in mice. *Blood*. 2011;118(15):4224–4230.
20. **Papanikolaou G, Samuels ME, Ludwig EH, et al.** Mutations in HFE2 cause iron overload in chromosome 1q-linked juvenile hemochromatosis. *Nat Genet*. 2004;36(1):77–82.
21. **Babitt JL, Huang FW, Wrighting DM, et al.** Bone morphogenetic protein signaling by hemojuvelin regulates hepcidin expression. *Nat Genet*. 2006;38(5):531–539.
22. **Niederkofler V, Salie R, Arber S.** Hemojuvelin is essential for dietary iron sensing, and its mutation leads to severe iron overload. *J Clin Invest*. 2005;115(8):2180–2186.
23. **Huang FW, Pinkus JL, Pinkus GS, Fleming MD, Andrews NC.** A mouse model of juvenile hemochromatosis. *J Clin Invest*. 2005;115(8):2187–2191.
24. **Kautz L, Meynard D, Monnier A, et al.** Iron regulates phosphorylation of Smad1/5/8 and gene expression of Bmp6, Smad7, Id1, and Atoh8 in the mouse liver. *Blood*. 2008;112(4):1503–1509.
25. **Corradini E, Meynard D, Wu Q, et al.** Serum and liver iron differently regulate the bone morphogenetic protein 6 (BMP6)-SMAD signaling pathway in mice. *Hepatology*. 2011;54(1):273–284.
26. **Casanovas G, Mleczko-Sanecka K, Altamura S, Hentze MW, Muckenthaler MU.** Bone morphogenetic protein (BMP)-responsive elements located in the proximal and distal hepcidin promoter are critical for its response to HJV/BMP/SMAD. *J Mol Med (Berl)*. 2009;87(5):471–480.
27. **Truksa J, Lee P, Beutler E.** Two BMP responsive elements, STAT, and bZIP/HNF4/COUP motifs of the hepcidin promoter are critical for BMP, SMAD1, and HJV responsiveness. *Blood*. 2009;113(3):688–695.
28. **Goumans MJ, Valdimarsdottir G, Itoh S, Rosendahl A, Sideras P, ten Dijke P.** Balancing the activation state of the endothelium via two distinct TGF-β type I receptors. *EMBO J*. 2002;21(7):1743–1753.
29. **Daly AC, Randall RA, Hill CS.** Transforming growth factor β-induced Smad1/5 phosphorylation in epithelial cells is mediated by novel receptor complexes and is essential for anchorage-independent growth. *Mol Cell Biol*. 2008;28(22):6889–6902.
30. **Wrighton KH, Lin X, Yu PB, Feng XH.** Transforming growth factor β can stimulate Smad1 phosphorylation independently of bone morphogenic protein receptors. *J Biol Chem*. 2009;284(15):9755–9763.
31. **Murakami M, Kawachi H, Ogawa K, Nishino Y, Funaba M.** Receptor expression modulates the specificity of transforming growth factor-β signaling pathways. *Genes Cells*. 2009;14(4):469–482.
32. **Liu IM, Schilling SH, Knouse KA, Choy L, Derynck R, Wang XF.** TGFβ-stimulated Smad1/5 phosphorylation requires the ALK5 L45 loop and mediates the pro-migratory TGFβ switch. *EMBO J*. 2009;28(2):88–98.
33. **Wang Y, Ho CC, Bang E, et al.** Bone morphogenetic protein 2 stimulates noncanonical SMAD2/3 signaling via the BMP type 1A receptor in gonadotrope-like cells: implications for FSH synthesis. *Endocrinology*. 2014;155(5):1970–1981.
34. **Holtzhausen A, Golzio C, How T, et al.** Novel bone morphogenetic protein signaling through Smad2 and Smad3 to regulate cancer progression and development. *FASEB J*. 2014;28(3):1248–1267.
35. **Schneyer AL, Sidis Y, Gulati A, Sun JL, Keutmann H, Krasney PA.** Differential antagonism of activin, myostatin and growth and differentiation factor 11 by wild-type and mutant follistatin. *Endocrinology*. 2008;149(9):4589–4595.
36. **Kim A, Fung E, Parikh SG, et al.** A mouse model of anemia of inflammation: complex pathogenesis with partial dependence on hepcidin. *Blood*. 2014;123(8):1129–1136.
37. **Xia Y, Babitt JL, Sidis Y, Chung RT, Lin HY.** Hemojuvelin regulates hepcidin expression via a selective subset of BMP ligands and re-

ceptors independently of neogenin. *Blood*. 2008;111(10):5195–5204.
38. **Xia Y, Babitt JL, Bouley R, et al.** Dragon enhances BMP signaling and increases transepithelial resistance in kidney epithelial cells. *J Am Soc Nephrol*. 2010;21(4):666–677.
39. **Korchynskyi O, ten Dijke P.** Identification and functional characterization of distinct critically important bone morphogenetic protein-specific response elements in the Id1 promoter. *J Biol Chem*. 2002;277(7):4883–4891.
40. **Zilberberg L, ten Dijke P, Sakai LY, Rifkin DB.** A rapid and sensitive bioassay to measure bone morphogenetic protein activity. *BMC Cell Biol*. 2007;8:41.
41. **Dennler S, Itoh S, Vivien D, ten Dijke P, Huet S, Gauthier JM.** Direct binding of Smad3 and Smad4 to critical TGF β-inducible elements in the promoter of human plasminogen activator inhibitor-type 1 gene. *EMBO J*. 1998;17(11):3091–3100.
42. **Zumbrennen-Bullough KB, Wu Q, Core AB, et al.** MicroRNA-130a is up-regulated in mouse liver by iron deficiency and targets the bone morphogenetic protein (BMP) receptor ALK2 to attenuate BMP signaling and hepcidin transcription. *J Biol Chem*. 2014;289(34):23796–2808.
43. **Fujikura Y, Krijt J, Nečas E.** Liver and muscle hemojuvelin are differently glycosylated. *BMC Biochem*. 2011;12:52.
44. **Rasband WS.** *1997–2012. ImageJ*. Bethesda, MD: National Institutes of Health. Available from: http://imagej.nih.gov/ij/.
45. **Meynard D, Vaja V, Sun CC, et al.** Regulation of TMPRSS6 by BMP6 and iron in human cells and mice. *Blood*. 2011;118(3):747–756.
46. **Wu Q, Sun CC, Lin HY, Babitt JL.** Repulsive guidance molecule (RGM) family proteins exhibit differential binding kinetics for bone morphogenetic proteins (BMPs). *PLoS One*. 2012;7(9):e46307.
47. **Tsuchida K, Nakatani M, Yamakawa N, Hashimoto O, Hasegawa Y, Sugino H.** Activin isoforms signal through type I receptor serine/threonine kinase ALK7. *Mol Cell Endocrinol*. 2004;220(1–2):59–65.
48. **Rejon CA, Hancock MA, Li YN, Thompson TB, Hébert TE, Bernard DJ.** Activins bind and signal via bone morphogenetic protein receptor type II (BMPR2) in immortalized gonadotrope-like cells. *Cell Signal*. 2013; 25(12):2717–2726.
49. **Constante M, Wang D, Raymond VA, Bilodeau M, Santos MM.** Repression of repulsive guidance molecule C during inflammation is independent of Hfe and involves tumor necrosis factor-α. *Am J Pathol*. 2007;170(2):497–504.
50. **Krijt J, Frýdlová J, Kukačková L, et al.** Effect of iron overload and iron deficiency on liver hemojuvelin protein. *PLoS One*. 2012;7(5):e37391.
51. **Sidis Y, Mukherjee A, Keutmann H, Delbaere A, Sadatsuki M, Schneyer A.** Biological activity of follistatin isoforms and follistatin-like-3 is dependent on differential cell surface binding and specificity for activin, myostatin, and bone morphogenetic proteins. *Endocrinology*. 2006;147(7):3586–3597.
52. **Deschemin JC, Vaulont S.** Role of hepcidin in the setting of hypoferremia during acute inflammation. *PLoS One*. 2013;8(4):e61050.
53. **Guida C, Altamura S, Klein FA, et al.** A novel inflammatory pathway mediating rapid hepcidin-independent hypoferremia. *Blood*. 2015;125(14):2265–2275.
54. **Jones KL, Mansell A, Patella S, et al.** Activin A is a critical component of the inflammatory response, and its binding protein, follistatin, reduces mortality in endotoxemia. *Proc Natl Acad Sci USA*. 2007;104(41):16239–1644.
55. **Feng XH, Derynck R.** Specificity and versatility in tgf-β signaling through Smads. *Annu Rev Cell Dev Biol*. 2005;21:659–693.